

Transcranial cavitation-mediated ultrasound therapy at sub-MHz frequency *via* temporal interference modulation

Cite as: Appl. Phys. Lett. **111**, 163701 (2017); <https://doi.org/10.1063/1.5000896>

Submitted: 19 August 2017 . Accepted: 01 October 2017 . Published Online: 16 October 2017

Tao Sun, Jonathan T. Sutton, Chanikarn Power, Yongzhi Zhang, Eric L. Miller, and Nathan J. McDannold



View Online



Export Citation



CrossMark

ARTICLES YOU MAY BE INTERESTED IN

[Feasibility of noninvasive cavitation-guided blood-brain barrier opening using focused ultrasound and microbubbles in nonhuman primates](#)

Applied Physics Letters **98**, 163704 (2011); <https://doi.org/10.1063/1.3580763>

[Microbubble mediated dual-frequency high intensity focused ultrasound thrombolysis: An In vitro study](#)

Applied Physics Letters **110**, 023703 (2017); <https://doi.org/10.1063/1.4973857>

[Generating arbitrary ultrasound fields with tailored optoacoustic surface profiles](#)

Applied Physics Letters **110**, 094102 (2017); <https://doi.org/10.1063/1.4976942>



Webinar
How to Characterize Magnetic Materials Using Lock-in Amplifiers

Zurich Instruments MFLI

Zurich Instruments

CRYOGENIC

Register now

Transcranial cavitation-mediated ultrasound therapy at sub-MHz frequency *via* temporal interference modulation

Tao Sun,^{1,2,a)} Jonathan T. Sutton,¹ Chanikarn Power,¹ Yongzhi Zhang,¹ Eric L. Miller,² and Nathan J. McDannold¹

¹*Focused Ultrasound Laboratory, Department of Radiology, Brigham and Women's Hospital, Harvard Medical School, Boston, Massachusetts 02115, USA*

²*Department of Electrical and Computer Engineering, Tufts University, Medford, Massachusetts 02155, USA*

(Received 19 August 2017; accepted 1 October 2017; published online 16 October 2017)

Sub-megahertz transmission is not usually adopted in pre-clinical small animal experiments for focused ultrasound (FUS) brain therapy due to the large focal size. However, low frequency FUS is vital for preclinical evaluations due to the frequency-dependence of cavitation behavior. To maximize clinical relevance, a dual-aperture FUS system was designed for low-frequency (274.3 kHz) cavitation-mediated FUS therapy. Combining two spherically curved transducers provides significantly improved focusing in the axial direction while yielding an interference pattern with strong side lobes, leading to inhomogeneously distributed cavitation activities. By operating the two transducers at slightly offset frequencies to modulate this interference pattern over the period of sonication, the acoustic energy was redistributed and resulted in a spatially homogenous treatment profile. Simulation and pressure field measurements in water were performed to assess the beam profiles. In addition, the system performance was demonstrated *in vivo* in rats *via* drug delivery through microbubble-mediated blood-brain barrier disruption. This design resulted in a homogenous treatment profile that was fully contained within the rat brain at a clinically relevant acoustic frequency. *Published by AIP Publishing.* <https://doi.org/10.1063/1.5000896>

Cavitation-mediated focused ultrasound (FUS) therapy is a promising method of drug delivery or tissue ablation without incision or ionizing radiation. Once administered intravenously or induced by high intensity exposures, cavitation seeds (micron-size bubbles) interact strongly with an ultrasound field. These microbubbles re-radiate the incident waves, localizing and amplifying the mechanical effects onto the targeted area. Various beneficial biological effects can thus be facilitated, including drug delivery *via* trans-cellular and/or cellular permeability enhancement [blood-brain barrier disruption (BBBD),¹⁻⁴ sonoporation⁵], thrombolysis,⁶ or non-thermal ablation.^{7,8} Of specific interest in this paper is the application of this technique to problems of drug delivery in the brain.

Many small animal investigations on FUS brain therapy have utilized a single-element transducer operating at a frequency of 1 MHz or higher for BBBD and other cavitation-mediated therapies. However, current clinically adopted transcranial FUS systems operate in the sub-megahertz range [for example, the Exablate Neuro Low Frequency (INSIGHTEC Ltd., Israel), which operates at 230 kHz]⁹ in order to minimize aberration and attenuation from the human skull. Such a low frequency is not typically adopted in small animal experiments^{2,10,11} due to the elongated focal area, leading to internal reflections and standing waves.¹²

Pre-clinical investigation in this sub-megahertz frequency range is vital because the cavitation behavior of microbubbles and corresponding bioeffects may vary as a function of FUS frequency.^{13,14} Therefore, the frequency mismatch between the pre-clinical and clinical setup may result in different treatment windows—the acoustic input range where microbubbles

undergo the appropriate cavitation regime (i.e., stable or inertial) for the therapy of interest.

To enable clinically relevant results in preclinical studies, we designed a low-frequency (274.3 kHz) FUS setup for small animal investigations. Two spherically curved transducers were combined to double the effective aperture size and provided significantly improved focusing in the axial direction. We operated the two apertures at slightly offset frequencies to modulate the interference pattern at the focal area. This design, along with the resulting temporal amplitude modulation at the difference (beat) frequency, produces a homogenous treatment profile that was contained within the rat brain in a clinically adopted frequency range. Simulation, acoustic field measurements in water, and drug delivery *in vivo* through BBBD in rats were performed to assess the performance of this system.

The dual-transducer system for FUS transmission was designed and built in-house. The system [Fig. 1(a)] consists of two air-backed, spherically focused transducers (diameter: 10 cm; focal length: 8 cm) with a resonant frequency at 274.3 kHz. The transducers were mounted in an acrylic holder at an angle of 102° with respect to each other (an angle greater than 90° was used to maximize the space between

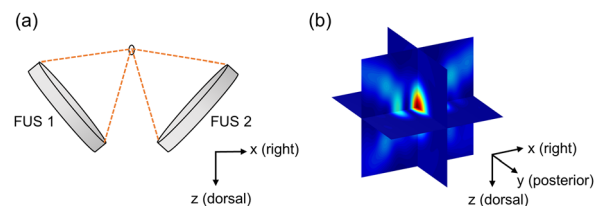


FIG. 1. Focused ultrasound system and beam profiles. (a) Illustration of the dual-aperture focused ultrasound setup. (b) Acoustic beam cross-sections of three orthogonal planes in the focal region.

^{a)} Author to whom correspondence should be addressed: taosun@bwh.harvard.edu

the transducers for a cavitation detector or imaging probe). To mitigate the interference pattern in the focal region, one of the transducers was operated at a frequency of 31 Hz higher than the other. At each point in the focal region, the pressure field was modulated over time at this frequency with a spatially varying phase offset. A frequency difference of 31 Hz was selected so that integration of the modulation envelope over one half of a period was close to that of the 10-ms burst applied at a single frequency commonly used for BBBD and nonthermal ablation. The burst length was one period of the difference frequency (32.3 ms), and the bursts were applied at a pulse repetition frequency (PRF) of 4 Hz. The pair of FUS transducers were driven by two function generators (33220A, Agilent, Santa Clara, CA, USA) and two amplifiers (43 dB gain, LZY-22+, Mini-Circuits, Brooklyn, NY, USA). The transducers were matched to 50 Ohms, and the electrical power output was measured using a power meter (E4419 B, Agilent) and a dual-directional coupler (C5948-10, Werlatone, Patterson, NY, USA). The transducers were calibrated using scans of the focal plane acquired with a needle hydrophone (HNC-1000, Onda, Sunnyvale, CA, USA) and radiation force balance measurements to estimate the peak intensity at the focus. The pressure amplitude at the combined focus of the two transducers was estimated from the needle hydrophone after calibrating it by driving one transducer and placing a needle hydrophone at its focus. Simulation of the acoustic field was performed using the fast near field method¹⁵ in FOCUS (Fast Object-oriented C++ Ultrasound Simulator, <http://www.egr.msu.edu/~fultras-web/>) and executed by a self-developed MATLAB (MathWorks, Natick, MA, USA) script. The mesh size was $\lambda/16$, where λ refers to the wavelength of ultrasound.

Operated individually, each aperture would generate a focus with axial dimensions larger than the rat brain. Simulations suggested that the resulting intensity field would have an axial full width at half maximum (FWHM) of 22.0 mm and a lateral FWHM of 5.1 mm [Fig. 2(a) left, and Fig. 3 in blue]. The combined focus of two crossing focal regions was used previously to reduce the focus size in the axial direction for ultrasound thermal therapy.¹⁶ However, simultaneous transmission at a single frequency results in an interference pattern in the focal region. In thermal therapy, this pattern can be mediated since thermal conduction will fill in the gaps. However, in cavitation-mediated therapies where the resulting bioeffects will follow the pressure distribution, this pattern will result in inhomogeneous drug delivery or ablation. The interference pattern was evident in our system in both simulations [Fig. 2(b), top] and maps of the acoustic intensity in degassed water [Fig. 2(c), top].

To disrupt the interference pattern and produce a spatially homogenous treatment profile, we drove each FUS source with a slightly different frequency ($\Delta f = 31$ Hz), causing the interference pattern to modulate over time (see [supplementary material](#) movies). With a burst length long enough to allow for one period at the beat frequency (32 ms), each point in the combined focal region received a full cycle of modulation. Both simulations and maps of the average pressure measured in water showed the expected homogeneous focal region [Figs. 2(b) and 2(c), bottom]. The axial dimension (FWHM: 5.9 and 6.4 mm, for simulations and measurements, respectively) of

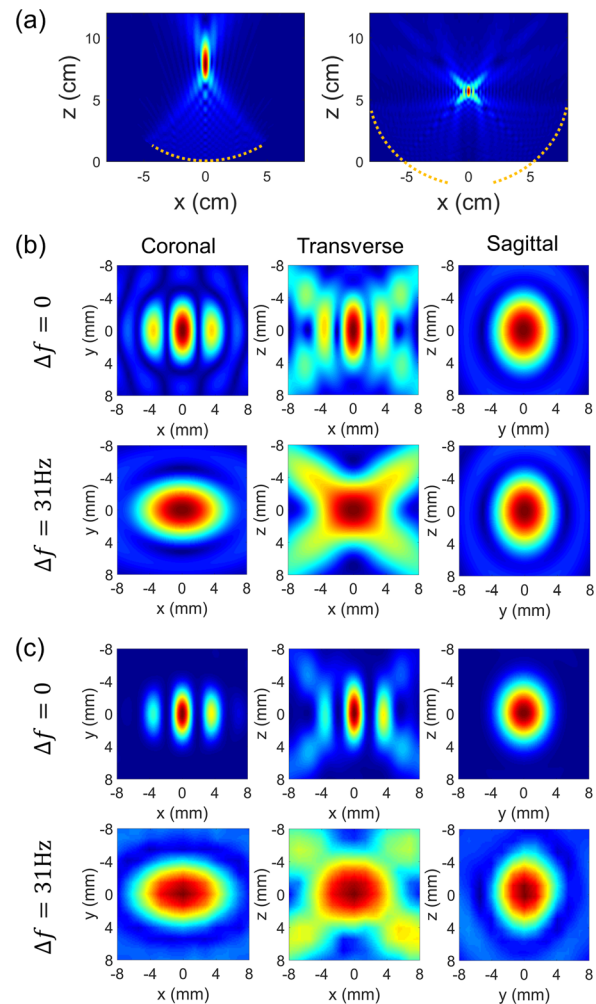


FIG. 2. Beam profile comparisons. (a) Simulated acoustic pressure fields of single-aperture (left) vs double-aperture (right) setups in the xz (transverse) plane. The dashed lines represent the aperture locations. (b) Simulated acoustic pressure field of the dual-aperture system for transmission at the same frequency ($\Delta f = 0$ Hz) and at two slightly different frequencies ($\Delta f = 31$ Hz). The coronal, transverse, and sagittal planes of these maps in the reference frame of the rat brain are indicated. (c) Measured acoustic pressure fields for transmission at the same frequency (top) and with a 31 Hz frequency difference (bottom). The time-averaged pressure obtained over a 32 ms burst is shown, and each map was normalized to the maximum pressure of each plane (shown on the linear scale). The “jet” colormap with a length of 64 was used (red: 1 and blue: 0).

the combined focus was less than the dorsal/ventral dimensions of the rat brain (approximately 1 cm), while the transverse dimensions (FWHM: 7.3×4.8 and 9.7×6.5 mm, for simulations and measurements, respectively) were slightly enlarged compared to the field of a single aperture. Figure 3 shows the normalized acoustic intensity profiles from a single transducer and for two transducers transmitting at the same frequency or with a 31-Hz frequency difference.

To further demonstrate the system performance for *in vivo* experiments, we disrupted the blood-brain barrier in Sprague Dawley rats (Charles River Laboratories, Inc., Wilmington, MA; ~ 300 g) and examined the corresponding distribution of Trypan Blue, a fluorescent model drug, using a fluorescent imaging system (constructed in-house). All animal experiments performed here were approved by Harvard Medical School Institutional Animal Care and Use Committees. Figure 4(a) shows the Trypan Blue distribution after FUS transmissions at

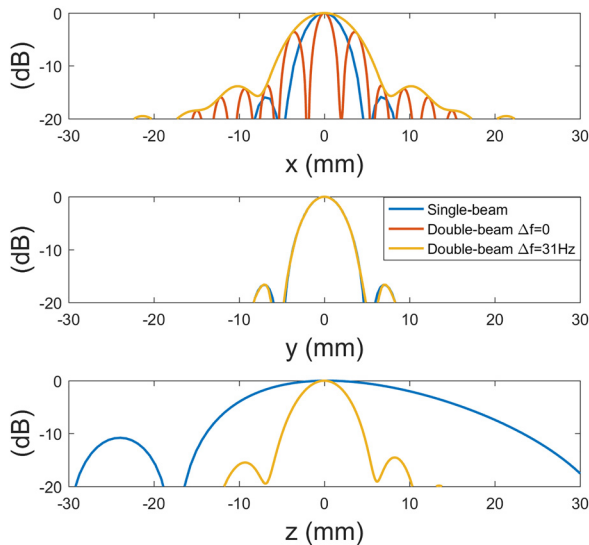


FIG. 3. Simulated peak normalized acoustic intensity profiles for transmission from a single aperture (in blue), two transducers at the same frequency (in orange), and two apertures with a 31 Hz frequency difference (in yellow).

the same frequency. Two targets were sonicated in succession, one in each hemisphere 1.5 mm lateral to the midline. Contours superimposed on the images (dotted lines: 90%; solid lines: 75%; dashed lines: 50% peak pressure) show the simulated pressure field distribution. They matched well with the resulting distribution of the tracer delivered to the brain. The distance between the main lobe and the side lobe in the drug delivery map was ~ 3.5 mm, corresponding well with the simulated distance of 3.54 mm shown in Fig. 3 (x direction).

For comparison, Fig. 4(b) shows the tracer distribution when two frequencies were used. In this example, which was part of a separate, ongoing study, we sonicated a tumor in

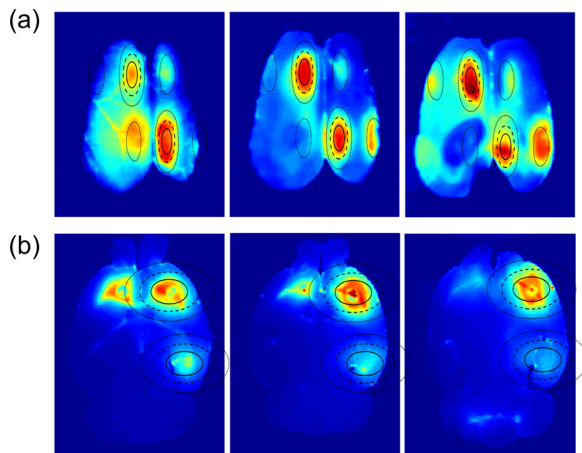


FIG. 4. Fluorescence imaging showing the distribution of a model drug after FUS-induced BBBB *in vivo* using transmissions (a) at the same frequency and (b) with 31-Hz frequency offset. The superimposed contours show the distribution of the simulated pressure fields at 90% (dotted lines), 75% (solid lines), and 50% (dashed lines) of the peak pressure. Images were taken from three consecutive 1-mm horizontal sections of the brains. Fluorescent intensities shown were in arbitrary units but fixed across the three sections in each animal. In this example, two targets were sonicated in succession, one in each hemisphere. In (b), glioma cells were implanted bilaterally in the striatum areas, resulting in some drug leakage on the unsonicated (left) side. Here, two targets were sonicated in succession in one hemisphere, one centered on the tumor and the other centered on the (non-tumor-bearing) hippocampus.

addition to a location in the healthy brain. Here, F98 glioma cells were implanted in the striatum in both hemispheres. Two separate sonications were then performed on one of the tumors and at another non-tumor location in the hippocampus. The drug leakage evident on the unsonicated (left) side resulted from the leaky vasculature of brain tumor. The resulting BBBB was localized, demonstrating the homogeneous combined focal region produced by this system. These results demonstrate that the proposed approach is able to achieve sub-centimeter axial treatment profiles in a tumor and in locations relevant for models of Parkinson's disease (striatum) and Alzheimer's disease (hippocampus). Detailed *in vivo* experiment protocols can be found in our previous publications.²

Overall, the proposed system has been shown to tighten the typical elongated ellipsoidal focus produced by single-aperture transducers, enabling the delivered drug distribution or non-thermal lesion to be confined within the rat brain at 274.3 kHz. The increased geometric gain of the combined system reduces the impact of internal reflections and standing waves, avoids affecting healthy tissue in the beam path, and improves the precision of treatment. In addition, it improves confidence for cavitation monitoring and control by minimizing the acoustic emissions arising in extracranial regions.

A potential limitation of this approach is that both sides of the brain are in the beam path. If the exposure level is too high, unwanted cavitation activity in the beam path could cause unwanted bio-effects, which would not be ideal if the contralateral hemisphere is used as a control. However, since the pressure levels along the two beam paths before reaching the combined focal area are lower than those of a single beam with the same focal pressure, the likelihood of undesired cavitation activity in the beam path should be lower than that of the single beam approach. An additional potential concern is that using two frequencies could alter the microbubble activity. For example, Suo *et al.*¹⁷ found an enhanced inertial cavitation effect when exciting microbubbles from two sources with two distinct frequencies. Such effects were not evident in our experiments. The possible reason could be that the frequency difference from the two sources in our approach is so small that the cavitation behaviors from microbubbles are still mainly characterized by the frequency of 274.3 kHz, or our cavitation detector might not be sensitive enough for capturing the slightly varied activities.

See [supplementary material](#) (videos) for the temporal interference pattern migration over the course of sonication. Instantaneous (left) and maximum (right) pressures measured in water are shown in the xy (coronal) plane.

This work was supported by National Institutes of Health Grant No. P01 CA174645. The authors would like to thank Dr. Rolf F. Barth (Department of Pathology, The Ohio State University, Columbus, OH 43210, USA) for providing the F98 cells and Mr. Yiqun Yang for the helpful discussions of performing acoustic pressure simulation in FOCUS. A provisional patent describing the focused ultrasound system developed in this work has been filed (inventors: N.J.M. and T.S.). N.J.M. holds another two published patents on the

ultrasound technique evaluated in this work. No conflicts of interest were disclosed by the other authors.

- ¹K. Hynynen, N. McDannold, N. Vykhodtseva, and F. A. Jolesz, *Radiology* **220**, 640 (2001).
- ²M. Aryal, C. D. Arvanitis, P. M. Alexander, and N. McDannold, *Adv. Drug Delivery Rev.* **72**, 94 (2014).
- ³S. Wang, O. O. Olumolade, T. Sun, G. Samiotaki, and E. E. Konofagou, *Gene Ther.* **22**, 104 (2015).
- ⁴C.-Y. Lin, H.-Y. Hsieh, C.-M. Chen, S.-R. Wu, C.-H. Tsai, C.-Y. Huang, M.-Y. Hua, K.-C. Wei, C.-K. Yeh, and H.-L. Liu, *J. Controlled Release* **235**, 72 (2016).
- ⁵Z. Fan, H. Liu, M. Mayer, and C. X. Deng, *Proc. Natl. Acad. Sci. U.S.A.* **109**, 16486 (2012).
- ⁶Y. Lu, J. Wang, R. Huang, G. Chen, L. Zhong, S. Shen, C. Zhang, X. Li, S. Cao, W. Liao *et al.*, *Stroke* **47**, 1344 (2016).
- ⁷N. J. McDannold, N. I. Vykhodtseva, and K. Hynynen, *Radiology* **241**, 95 (2006).
- ⁸K.-W. Lin, T. L. Hall, Z. Xu, and C. A. Cain, *Ultrasound Med. Biol.* **41**, 2148 (2015).
- ⁹Y. Huang, R. Alkins, M. Chapman, J. Perry, A. Sahgal, M. Trudeau, T. Mainprize, and K. Hynynen, *Proc. Intl. Magn. Reson. Med.* **24**, 450 (2016), see <http://dev.ismrm.org/2016/0450.html>.
- ¹⁰A. Burgess and K. Hynynen, *ACS Chem. Neurosci.* **4**, 519 (2013).
- ¹¹T. Sun, G. Samiotaki, S. Wang, C. Acosta, C. C. Chen, and E. E. Konofagou, *Phys. Med. Biol.* **60**, 9079 (2015).
- ¹²M. A. O'Reilly, Y. Huang, and K. Hynynen, *Phys. Med. Biol.* **55**, 5251 (2010).
- ¹³K. B. Bader and C. K. Holland, *Phys. Med. Biol.* **58**, 127 (2013).
- ¹⁴N. McDannold, N. Vykhodtseva, and K. Hynynen, *Ultrasound Med. Biol.* **34**, 834 (2008).
- ¹⁵J. F. Kelly and R. J. McGough, *AIP Conf. Proc.* **1113**, 210 (2009).
- ¹⁶X. Chen, P. Novák, D. G. Benson, J. S. Webber, L. Hennings, G. Shafirstein, P. M. Corry, R. J. Griffin, and E. G. Moros, *Med. Phys.* **38**, 1877 (2011).
- ¹⁷D. Suo, Z. Jin, X. Jiang, P. A. Dayton, and Y. Jing, *Appl. Phys. Lett.* **110**, 023703 (2017).